Physics of the Solid State, Vol. 43, No. 8, 2001, pp. 1522–1526. Translated from Fizika Tverdogo Tela, Vol. 43, No. 8, 2001, pp. 1462–1466.

MAGNETISM AND FERROELECTRICITY

Ferromagnetic and Spin-Wave Resonance in $Ni_{0.8}Fe_{0.2}/Dy_{1-x}Co_x$ Bilayer Films

R. S. Iskhakov*, V. Yu. Yakovchuk*, S. V. Stolyar, L. A. Chekanova*, and V. A. Seredkin***

** Kirensky Institute of Physics, Siberian Division, Russian Academy of Sciences, Akademgorodok, Krasnoyarsk, 660036 Russia*

*** Krasnoyarsk State University, Krasnoyarsk, 660041 Russia*

e-mail: rauf@iph.krasnoyarsk.su

Received November 1, 2000

Abstract—The standing spin wave spectra of $Ni_{0.8}Fe_{0.2}$(1000–3000 Å)/($Dy_{1-x}Co_x$(700 Å) bilayer exchange-biased films with two different (precompensation $Dy_{0.2}Co_{0.8}$ and postcompensation $Dy_{0.3}Co_{0.7}$) compositions of the hard magnetic layer are analyzed. Measurements are performed at room temperature. It is found that the effective magnetic layer thickness ($d_{eff} = d_0 \pm \Delta d$), which determines the wave vectors of the first modes in the spectrum, differs from the d_0 value specified in film technology. The sign of $|\Delta d| \sim 500$ Å is governed by the composition of the DyCo hard magnetic layer. © *2001 MAIK "Nauka/Interperiodica".*

1. INTRODUCTION

Intensive studies of exchange-biased films of the soft magnetic ferromagnet–hard magnetic ferrimagnet (antiferromagnet) type are stimulated by the modern demand for microelectronics [1]. In the present work, we examined the dynamic magnetic characteristics in order to determine the parameters of ferromagnetic resonance (FMR) and spin-wave resonance (SWR) in bilayer films of the compositions $Ni_{0.8}Fe_{0.2}/Dy_{0.2}Co_{0.8}$ and $Ni_{0.8}Fe_{0.2}/Dy_{0.3}Co_{0.7}$. The choice of these compositions of the rare-earth metal–transition metal amorphous ferrimagnetic alloy was made for the following reasons. It is known that DyCo amorphous alloys prepared in the form of solid solutions over a wide range of concentrations are characterized by a point of magnetic compensation. For example, the $Dy_{0.23}Co_{0.77}$ amorphous alloy is compensated at room temperature. The rare-earth metal–transition metal alloy compositions chosen for our investigations lie on different sides of the compensation point on the composition axis and, at the same time, are characterized by close magnitudes of magnetic characteristics, such as the saturation magnetization M_s= 80 G, the coercive force $H_c \sim 4$ kOe, and the perpendicular magnetic anisotropy $K = 3 \times 10^5$ erg/cm^3 [2].

Analysis of the spin wave spectra of these bilayer films revealed a very interesting effect associated with the exchange interaction between the ferromagnet–ferrimagnet layers. It was found that resonance fields of the first modes of the standing spin waves excited by microwave fields in a permalloy layer substantially depend on the chemical composition of the hard magnetic layer. The present paper reports the results of detailed investigation into this phenomenon.

2. SAMPLE PREPARATION AND EXPERIMENTAL TECHNIQUE

The NiFe/DyCo bilayer exchange-biased films were prepared by thermal evaporation under vacuum (3×10^{-6} mmHg). Cover glasses were used as substrates. The layers were deposited from three independent evaporators with a ring cathode. The permalloy layer was deposited in a constant magnetic field (20 Oe) applied along the sample plane. The thickness of the $Ni_{0.8}Fe_{0.2}$ layer was varied from 1000 to 3000 Å. The thickness of the DyCo hard magnetic layer was equal to 700 Å. Sufficiently low substrate temperatures (≤50°C), which were observed during film deposition, and the amorphous state of the hard magnetic layer (as is known, the diffusion coefficient for amorphous alloys is considerably less than that for their crystal analogues) allowed us to conclude that the studied films had a clearly defined interface between the ferromagnet–ferrimagnet layers. The magnetooptical Kerr effect in fields up to 15 kOe was used as a test technique for determining the precompensation or postcompensation composition of the hard magnetic layer. Figure 1 shows the typical magnetooptical hysteresis loops measured for the $Dy_{0.2}Co_{0.8}$ and $Dy_{0.3}Co_{0.7}$ alloy films. In order to prevent oxidation of the hard magnetic layer, a protective GeO layer was deposited onto the DyCo layer or the reversed sequence of layers DyCo/NiFe was used.

The dynamic magnetic properties of the $Ni_{0.8}Fe_{0.2}/Dy_{0.2}Co_{0.8}$ and $Ni_{0.8}Fe_{0.2}/Dy_{0.3}Co_{0.7}$ bilayer films were measured on a standard spectrometer operating in the *X* band (9.2 GHz). The FMR fields were measured at room temperature over the entire range of angles between the external field and the film plane with the aim of determining the effective magnetization

M_{eff}. The M_{eff} magnetization is defined by the relationship

$$H_{\perp}^{r} - 4\pi M_{\text{eff}} = \sqrt{H_{\parallel}^{r}(H_{\parallel}^{r} + 4\pi M_{\text{eff}})}, \quad (1)$$

where $H_{\perp}^{r}$ and $H_{\parallel}^{r}$ are the FMR fields at the appropriate geometry of the experiment.

The spin-wave resonance spectra were recorded perpendicular to the external magnetic field with respect to the plane of the studied films. For this geometry of the measurements, the resonance field H_n and the wave vector k_n of a standing spin wave are related by the following expression:

$$H_n = \omega/\gamma + 4\pi M_{\text{eff}} - \eta k_n^2, \quad (2)$$

where ω/γ is the internal field of a ferromagnet, $\eta = (2A/M_{\text{eff}})$ is the spin-wave stiffness, and A is the exchange coupling constant. As follows from the spin-wave resonance spectra (Fig. 2), the exchange boundary conditions for alternating magnetization are realized in the studied films. It is known that, in this case, the mode number n in the spin wave spectrum and the wave vector k_n of the standing spin wave are related by the formula $k_n = \pi n/d$ (where $n = 1, 2, 3, \ldots$ and d is the film thickness). By using expression (2), the numerical values of the spin-wave stiffness η were calculated from the relationship

$$\eta = (d/\pi)^2(H_i - H_j)/(n_j^2 - n_i^2). \quad (3)$$

The linewidth ΔH_n of the spin-wave mode was determined from the difference between the coordinates of extrema in the curve of the absorption spectrum derivative.

3. RESULTS

Before proceeding to the experimental results obtained for the $Ni_{0.8}Fe_{0.2}/Dy_{1-x}Co_x$ bilayer films, we recall that the $Ni_{0.8}Fe_{0.2}$ monolayer films 3000 Å thick were also prepared according to the above procedure. In the subsequent discussion, the magnetic characteristics and the spin-wave resonance spectra of the monolayer films will be used as reference data. The number of peaks observed in the spin-wave resonance spectra of these samples was greater than 10. The numerical values of the resonance fields H_n are approximated by a linear dependence in the $H_n(n^2)$ coordinates. The slope of this curve is determined by the spin-wave stiffness [see relationship (3)]. For $Ni_{81}Fe_{19}$ monolayer films, the calculated spin-wave stiffness η is equal to 20×10^{-10} Oe cm^2. The numerical values of the effective magnetization M_{eff} and the exchange coupling constant A are equal to 800 G and 0.8×10^{-6} erg/cm, respectively. The main magnetic characteristics, which were calculated for the $Ni_{0.8}Fe_{0.2}$ alloy, agree with those obtained by Rusov [3].

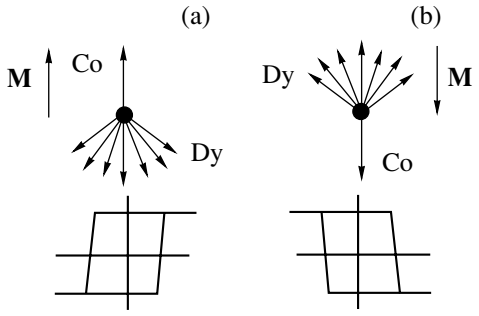

Fig. 1. A schematic representation of hypothetical local noncollinear magnetic structures of DyCo amorphous films and their typical magnetooptical hysteresis loops for (a) precompensation and (b) postcompensation alloy compositions.

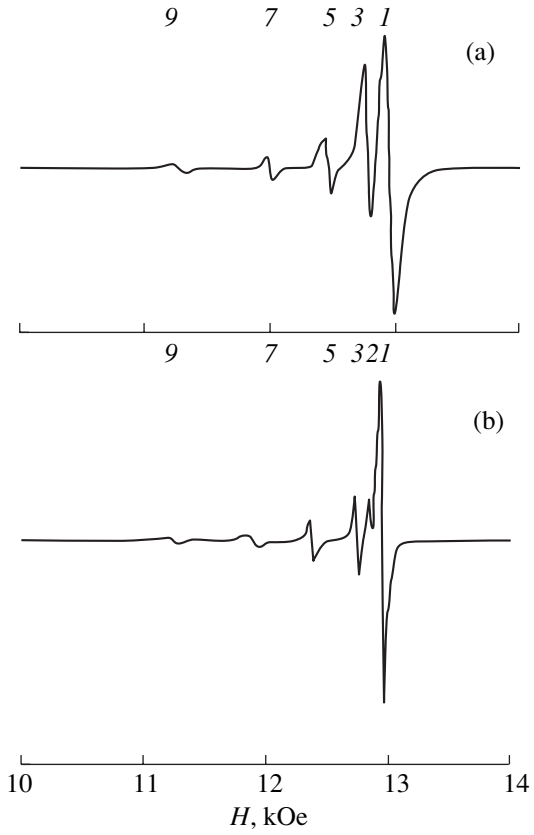

Fig. 2. Spin-wave resonance spectra of NiFe/DyCo bilayer films with (a) precompensation and (b) postcompensation hard magnetic layers.

Figure 2 shows the spin-wave resonance absorption spectra of NiFe/DyCo bilayer films, namely, the $Ni_{0.8}Fe_{0.2}/Dy_{0.2}Co_{0.8}$ film with a hard magnetic layer of the precompensation composition (Fig. 2a) and the $Ni_{0.8}Fe_{0.2}/Dy_{0.3}Co_{0.7}$ film with a hard magnetic layer of the postcompensation composition (Fig. 2b). Analysis of these spectra revealed the following features. (1) The spin-wave modes with odd and even numbers

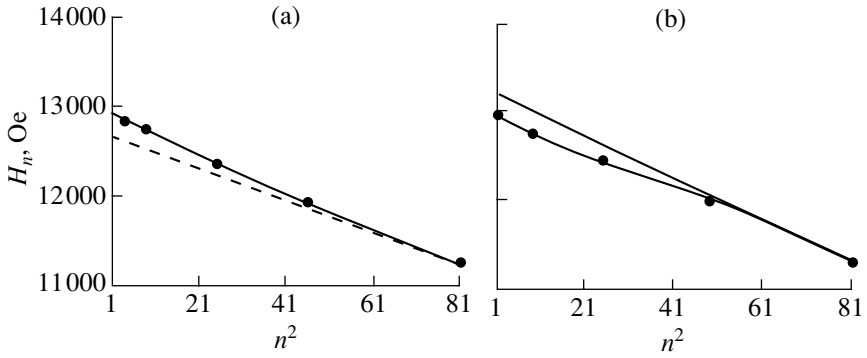

Fig. 3. Experimental dispersion dependences in the $H_n(n^2)$ coordinates for NiFe/DyCo bilayer films with (a) precompensation and (b) postcompensation hard magnetic layers.

($n = 1, 2, 3, \ldots$) are excited in the samples. (2) The intensities of even peaks are appreciably less than those of the neighboring odd peaks. (3) The intensities of even peaks in the spin-wave resonance spectra of bilayer films with a hard magnetic layer of the postcompensation composition (Fig. 2b) are considerably higher than those of the precompensation composition (Fig. 2a). The numerical values of the linewidth ΔH_1 in the spin wave spectra of these bilayer films also differ substantially. The linewidths ΔH_1 of the spin-wave resonance spectra of the studied films at different thicknesses of the permalloy layer and the effective magnetizations M_{eff} are listed in the table. From these data, it is seen that the magnetization M_{eff} of the bilayer films only slightly depends on the chemical composition of the hard magnetic layer. The deviations of the magnetization from the reference value of M_{eff} for the $Ni_{0.8}Fe_{0.2}$ alloy do not exceed 10%. At the same time, the linewidths ΔH_1 of the first mode in the spin-wave resonance spectra for the bilayer films with precompensation hard magnetic layers are twice (and more) as large as those for the films with postcompensation DyCo hard magnetic layers.

Linewidths ΔH_1 of the first mode in the spin-wave resonance spectra and effective magnetizations M_{eff} for NiFe/DyCo bilayer films

Precompensation composition of the DyCo alloy			
Parameter	NiFe (1000 Å) DyCo (700 Å)	NiFe (2000 Å) DyCo (700 Å)	NiFe (3000 Å) DyCo (700 Å)
ΔH_1, Oe	150	230	150
M_{eff}, G	724	727	800
Postcompensation composition of the DyCo alloy			
Parameter	NiFe (1500 Å) DyCo (700 Å)	NiFe (3000 Å) DyCo (700 Å)	NiFe (3000 Å) DyCo (700 Å)
ΔH_1, Oe	84	96	75
M_{eff}, G	727	810	850

Figure 3 depicts the experimental dispersion curves in the $H_n(n^2)$ coordinates for NiFe (3000 Å)/DyCo (700 Å) bilayer films with the same layer thicknesses but different (precompensation (Fig. 3a) or postcompensation (Fig. 3b)) compositions of the hard magnetic layer. The dashed line in Fig. 3 corresponds to the spin-wave stiffness $\eta \approx 20 \times 10^{-10}$ Oe cm^2, which was determined from the last modes in the spin-wave resonance spectra of these samples according to relationship (3). It should be noted that the exchange stiffness of bilayer films, which was calculated from the short-wavelength part of the spin wave spectra for both the precompensation and postcompensation alloy compositions of the hard magnetic layer, coincides with the reference value of η for the $Ni_{0.8}Fe_{0.2}$ monolayer film. However, as can be seen from Fig. 3, the resonance fields H_n of the first modes in the spin-wave resonance spectra are characterized by a systematic deviation from the reference dependence $H_n(n^2)$. In the case of bilayer films with precompensation hard magnetic layers, the measured fields H_n of the first modes in the spectrum exceed the reference values by δH_n (Fig. 3a). The opposite situation is observed in the films with postcompensation hard magnetic layers: the fields H_1, H_2, and H_3 are less than the reference values (Fig. 3b). It is also seen that an increase in the mode number n leads to a decrease in the magnitude of δH_n and, at $n = 5$, $\delta H_n \longrightarrow 0$.

As is known, the dispersion curves $H_n(n^2)$, which are calculated from the spin-wave resonance spectra of ferromagnetic films of disordered (amorphous, nanocrystalline, etc.) alloys, can exhibit specific features due to fluctuations of the magnetic parameters, the exchange interaction α [4], and the saturation magnetization M_s [5]. However, in our case, the feature observed in the $H_n(n^2)$ curve is caused by other factors. (This is evident, in particular, from a comparison of the $H_n(n^2)$ curves for the studied bilayer films and the $H_n(n^2)$ curve of the $Ni_{0.8}Fe_{0.2}$ reference film.) In our opinion, these are the interlayer exchange interaction and the orientation of

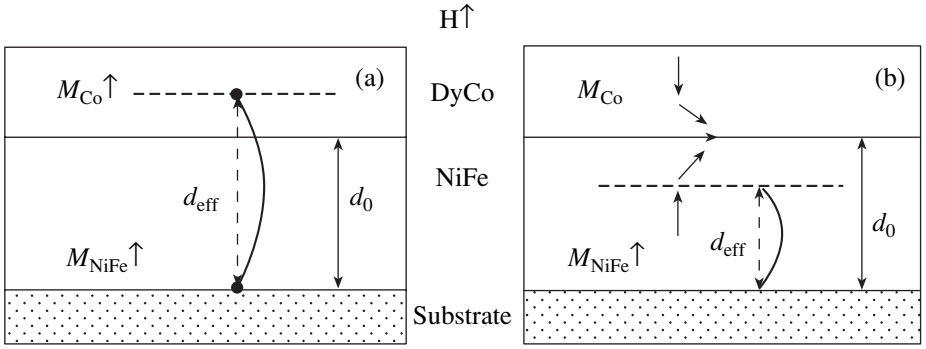

Fig. 4. Configurations of the magnetization vectors and thicknesses d_{eff} of effective magnetic layers in NiFe/DyCo bilayer films with (a) precompensation and (b) postcompensation hard magnetic layers.

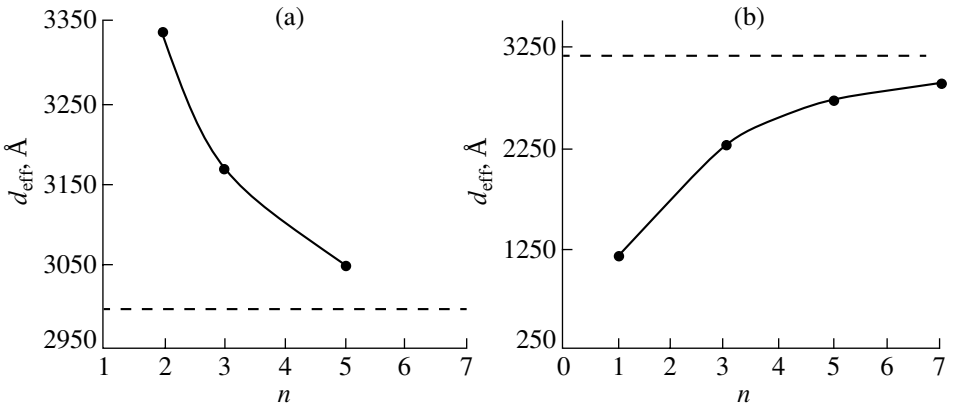

Fig. 5. Dependences of the effective magnetic thickness d_{eff} on the spin-wave mode number for NiFe/DyCo bilayer films with (a) precompensation and (b) postcompensation hard magnetic layers.

the Co sublattice magnetization in DyCo with respect to the external magnetic field **H**.

4. DISCUSSION

Let us consider the configuration of the magnetization vectors in the NiFe/DyCo bilayer films. For a bilayer film with the precompensation hard magnetic layer, the saturation magnetization vectors of the NiFe ferromagnetic alloy and the Co sublattice of the DyCo ferrimagnetic alloy are parallel to each other (Fig. 4). Owing to the exchange interaction between the local magnetic moments of the NiFe alloy and the local magnetic moments of Co atoms located near the interlayer boundary, the latter moments are involved in the precession of the net magnetization of the ferromagnetic layer under the effect of microwave fields. Hence, the exchange boundary condition for the alternating magnetization m (the Kittel condition $\mathbf{m}|_s = 0$), which specifies the node of a standing spin wave, should be met in a certain effective plane within the hard magnetic layer rather than at the interface. This is equivalent to the displacement of the standing spin wave node from the interface inside the $Dy_{0.2}Co_{0.8}$ hard magnetic alloy layer. (This situation is schematically shown in Fig. 4a). Therefore, in relationship (2), the wave vector of the first modes in the spin wave spectrum should be determined not from the formula $k_1 = \pi/d_0$ (where d_0 is the thickness of the permalloy film) but from the expression $k_1 = \pi/d_{eff}$ at $d_{eff} > d_0$ (where d_{eff} is the thickness of the effective magnetic layer for a spin wave).

The configuration of the magnetization vectors in a bilayer film with the postcompensation hard magnetic layer is depicted in Fig. 4b (see also Fig. 1b). In this case, the saturation magnetization vectors of the Co sublattice and the NiFe ferromagnetic alloy are antiparallel. The minimization of the energy (in the case of the exchange interaction Co $\longleftrightarrow$ NiFe and the uniaxial anisotropy of the DyCo hard magnetic layer) results in the formation of a transition layer between NiFe and DyCo in which spins of 3*d* metals gradually turn through an angle of π. Then, the Kittel exchange boundary condition in the interface region is replaced

by the Amenta–Rado boundary conditions $\left(\frac{\partial \mathbf{m}}{\partial \mathbf{n}}\right)_s = 0$, where **n** is the normal to the ferromagnet surface. This is confirmed by the increase in intensity of even peaks in the spin-wave resonance spectrum. Note that this configuration of free surface spins is realized in a certain effective plane inside the NiFe soft magnetic layer. This means that the thickness of the effective magnetic layer d_{eff}, which determines the wave vectors of the first spin-wave modes $k_1 = \pi/d_{\text{eff}}$), must satisfy the condition $d_{\text{eff}} < d_0$.

Numerical estimates of d_{eff} can be obtained using the relationship

$$\delta H_n/(\pi n)^2 = \eta[d_{\text{eff}}^{-2} - d_0^{-2}], \quad (4)$$

which is derived from formulas (2) and (3). The calculated dependences of the effective magnetic thickness d_{eff} on the spin-wave mode number for the studied bilayer films with precompensation and postcompensation hard magnetic layers are shown in Figs. 5a and 5b, respectively. It can be seen that, as the mode number n increases (the external magnetic field decreases), $d_{\text{eff}} = (d_0 \pm \Delta d)$ tends to d_0. Since $\Delta d \sim [(A + MH)/K]^{-0.5}$ (where K is the effective surface anisotropy constant for a layer of thickness Δd), a decrease in Δd with a decrease in the external magnetic field is quite reasonable. It is also important that the short-wavelength part of the spin-wave resonance spectrum depends only slightly on the type of exchange boundary conditions involved.

In conclusion, it should be noted that researchers dealing with the dynamic characteristics of thin metallic ferromagnetic films, apparently, rather frequently encounter the phenomenon described in the present work. Actually, thin metallic films prepared using different techniques undergo oxidation and, hence, are coated with ferrimagnetic (antiferromagnetic) oxides bound to the main ferromagnetic materials of these films through exchange interaction. For this reason, the deviations of the first peaks in the spin-wave resonance spectra from the dispersion dependence for spin waves are frequently observed. As a rule, the locations of these peaks are not included in subsequent analysis of the spin wave spectrum or their use leads to incorrect determination of the exchange coupling constant.

ACKNOWLEDGMENTS

We are grateful to S.A. Karpenko for helpful discussions.

REFERENCES

1. V. A. Seredkin, G. I. Frolov, and V. Yu. Yakovchuk, Pis'ma Zh. Tekh. Fiz. **9** (23), 1446 (1983) [Sov. Tech. Phys. Lett. **9**, 621 (1983)].
2. K. Handrich and S. Kobe, *Amorphe Ferro- und Ferrimagnetika* (Physik-Verlag, Weinheim, 1980; Mir, Moscow, 1982).
3. G. I. Rusov, Fiz. Tverd. Tela (Leningrad) **9**, 196 (1967) [Sov. Phys. Solid State **9**, 146 (1967)].
4. V. A. Ignatchenko, R. S. Iskhakov, L. A. Chekanova, and N. S. Chistyakov, Zh. Éksp. Teor. Fiz. **75** (2), 653 (1978) [Sov. Phys. JETP **48**, 328 (1978)].
5. R. S. Iskhakov, M. M. Brushtunov, and A. S. Chekanov, Fiz. Tverd. Tela (Leningrad) **29**, 1214 (1987) [Sov. Phys. Solid State **29**, 692 (1987)].

Translated by O. Borovik-Romanova